A Nonempirical Approach to Ground-State Jahn−Teller Distortion: Case Study of VCl_4[†]

Raf Bruyndonckx, Claude Daul,* and P. T. Manoharan

Institut de Chimie Inorganique et Analytique, CH 1700 Fribourg, Switzerland

Eric Deiss

Paul-Scherrer-Institut, CH 5232 Villigen, Switzerland

Received October 10, 1996[⊗]

A density functional based first-principles study of the Jahn−Teller (JT) distortion of VCl_4 is presented. The method used in this study includes an exploration of the adiabatic energy surface along the JT active mode as well as a full total energy relaxation along the path of minimal energy. The two approaches are shown to agree extremely well. A calculation of the JT stabilization energy with either method yields 51 cm^{-1} for the flattened tetrahedron and 40 cm^{-1} for the elongated conformation. For the JT-distortion a value of 0.08 Å is predicted. The results obtained in this work demonstrate once more the good ability of DFT calculations to predict the state energies as well as the corresponding structural parameters with a reasonable accuracy.

1. Introduction

The fundamental importance of the problem of electron−vibration interaction in the form of the Jahn−Teller (JT) effect as applied to transition metal complexes is well understood.[1−6] It is noted that most JT sensitive coordination compounds have an electronic degenerate or nearly degenerate term in the ground or first excited state. With a $d^1(T_d)$ or $d^9(O_h)$ or a $d^4(O_h)$ high-spin electronic configuration one of the e or e_g orbitals will be singly occupied and the complex will distort as a consequence of a first-order JT effect. The spectroscopic and kinetic properties of complex ions such as V^{4+} (d^1), Cr^{2+} (d^4), and Cu^{2+} (d^9) differ from those of neighboring ions of similar charge. Some of the spectroscopic techniques, especially electron spin resonance (ESR) and optical spectroscopy, have played a vital role in the experimental understanding of the presence, magnitude, and nature of the JT distortion in such metal complexes, though the experimental data are dominated by Cu^{2+} and to some extent Cr^{2+}.

Similarly, the literature is abundant with examples of JT distortion of excited states. The study of the JT distortion of low-lying excited states has relevance in photocatalytic, photochemical, and photosensitizer properties of coordination compounds. Such characteristic distortions and hence the removal of the degeneracy of JT sensitive states and their properties can be well understood by considering the potential energy surface as a function of nuclear coordinates. It is informative and useful to derive theoretically the JT energy E_{JT}—the depth of the minimum of the adiabatic potential surface relative to the regular configuration—as well as the nuclear displacement R_{JT}.

Though there is an abundance of quantum chemical studies on the molecular and electronic structures of metal ions and their complexes at various levels of sophistication, a nonempirical approach toward calculating such adiabatic potential surfaces arising out of JT distortion is rather limited. There have been attempts to study weak second-order JT effects of $[M(H_2O)_6]^{3+}$ (M = Zn, Cd, or Hg) using post-Hartree−Fock calculations and effective core potentials.[7] Also, the adiabatic potential energy surfaces for a ground-state, strong first-order E ⊗ e JT coupling in $[Cu(H_2O)_6]^{2+}$, $[Cr(H_2O)_6]^{2+}$, and $[Mn(H_2O)_6]^{3+}$ have been calculated by Akesson and co-workers[8] using SCF methodology. They performed an SCF calculation on the clusters of these hexaaquo ions in D_{2h} symmetry and also a correlated pair functional calculation on the first two of the three ions. No other computational attempt on first-order E ⊗ e JT coupling is known to have been performed on ground states, to the best of our knowledge, except for the crystal-field, ligand-field, and semiempirical MO based calculations on VCl_4.[9−11] These are all thus far the limited efforts on the theoretical attempts to understand the JT effect on the ground states of molecules.

It must, however, be said that quantum chemical calculations based on density functional theory (DFT) have been performed to elucidate the JT distortion of the excited states of a few molecules,[12−14] following the calculation of the multiplet splitting in DFT by Ziegler *et al*.[15] Since the multiplet states arising from open-shell configurations, such as the ones in JT sensitive coordination compounds, can in general not be

[†] This paper is dedicated to Alex von Zelewsky on the occasion of his 60th birthday.

[⊗] Abstract published in *Advance ACS Abstracts,* August 1, 1997.

(1) Bersuker, I. B. *The Jahn−Teller Effect and Vibronic Interactions in Modern Chemistry*, Plenum Press: London, 1984.
(2) Ballhausen, C. J. *Molecular Electronic Structures of Transition Metal Complexes*; McGraw-Hill: New York, 1979.
(3) Ballhausen, C. J. In *Vibronic Processes in Inorganic Chemistry*; Flint C. F., Ed.; Kluwer Academic Publishers: Dordrecht, 1989; pp 53−78.
(4) Bersuker, I. B. *Electronic Structure and Properties of Transition Metal Compounds*; John Wiley & Sons, Inc.: New York, 1996; Chapter 7.
(5) Bersuker, I. B.; Polinger, V. Z. *Vibronic Interactions in Molecules and Crystals* , Springer: Berlin, 1989.
(6) Perlin, Yu. E., Wagner, M., Eds. *The Dynamical Jahn−Teller Effect in Localised Systems*; North-Holland: Amsterdam, 1984.
(7) Strömberg, D.; Sandström, M.; Wahlgren, U. *Chem. Phys. Lett.* **1990**, *172*, 49.
(8) Akesson, R.; Pettersson, L. G. M.; Sandström, M.; Wahlgren, U. *J. Phys. Chem.* **1992**, *96*, 150.
(9) Ballhausen, C. J.; Liehr, A. D. *Acta Chem. Scand.* **1961**, *15*, 5.
(10) Lohr, L. L.; Liepscomb, W. N. *Inorg. Chem.* **1963**, *2*, 911.
(11) Ballhausen, C. J.; de Heer, J. *J. Chem. Phys.* **1965**, *43*, 4304.
(12) Daul, C.; Güdel, H.-U.; Weber, J. *J. Chem. Phys.* **1993**, *98*, 4023.
(13) Daul, C. *Int. J. Quantum Chem.* **1994**, *52*, 865.
(14) Gilardoni, F.; Weber, J.; Bellafrouh, K.; Daul, C.; Güdel, H.-U. *J. Chem. Phys.* **1996**, *104*, 7624.
(15) Ziegler, T.; Rank, A.; Baerends, E. J. *Theor. Chim. Acta* **1977**, *43*, 261.

S0020-1669(96)01220-7 CCC: $14.00

expressed by a single determinant, they have exploited the molecular symmetry to the largest possible extent to simplify the relation between multiplet splitting and single determinant energies. It is well-known that both classical Hartree−Fock theory and DFT exploit molecular symmetry. But the DF methods have certain advantages over the ones using HF because of the former's inclusion of correlation effects into the Hamiltonian via the exchange correlation functional and, according to our experience, its greater tractability when dealing with electronic structures of coordination compounds. Furthermore, the proposed treatment is based on nonempirical calculations. For these reasons, we thought of finding a simple recipe for the calculation of the ground-state JT stabilization energy and the resulting properties with the use of a nonempirical approach like that of DFT. In order to achieve this objective we have applied the suggested recipe on a simple JT molecule like VCl_4, whose properties have been extensively studied.

Among the simplest of the JT molecules is VCl_4, a tetrahedral $3d^1$ case, which is characterized by a moderate E ⊗ e JT coupling. The degenerate deformation vibration ν_2(E) would be strongly involved in vibronic interactions and would cause a distortion of the molecule from its ideal tetrahedral symmetry. Dilution of this molecule in a variety of tetrahedral (e.g., $TiCl_4$) and other host systems such as solvents, followed by ESR and other spectroscopic analysis, indicates that this exhibits a JT energy comparable to a vibrational quantum, $E_{JT} \sim \hbar\nu \sim 100$ cm^{-1}.[16−22] The axially symmetrical ESR parameters have been interpreted by the use of a vibronic ground state of the form

$$\Psi = \sin\alpha|3d_{z^2}\rangle\chi_I + \cos\alpha|3d_{x^2-y^2}\rangle\chi_{II}$$

with $\langle\chi_I|\chi_{II}\rangle = 0$ and the vibronic mixing angle being 54−59°. They are also to a large extent independent of the matrix employed. The weighted ratio of the two electronic wave functions has been found to be 3:1 in favor of stabilization under flattening rather than elongation as a result of a vibration-imposed D_{2d} structure.[22] However, Johannesen and co-workers found that the ground state of VCl_4 was a mixture of "58% flattened and 42% elongated configuration" (cit.).[18] ESR studies of polycrystalline VCl_4 in $TiCl_4$ indicate the presence of a potential barrier height of ∼18 cm^{-1} and a vibrational amplitude of 0.26 Å.[19] There seems to be a virtual absence of spin−orbit coupling between the two degenerate electronic wave functions.[21,22] The JT radius R_{JT} and energy E_{JT} have been calculated using extended Hückel molecular orbital theory to be respectively 0.032 Å and 6 cm^{-1}.[21] Morino and Uehara[17] report a V−Cl bond distance of 2.138(2) Å and estimate the ν_2(E) to be of the order of 108 cm^{-1} in comparison to 118 cm^{-1} of $TiCl_4$. They concluded from their experiments a JT energy of 73 (±43) cm^{-1} and a JT radius of 0.16(6) Å. The earlier calculations of Lohr and Lipscomb[10] and Ballhausen and de Heer[11] reveal that no static distortion from the tetrahedral geometry could be expected since the corresponding stabilization was less than the relevant vibrational energy. The zero-point energy and amplitude for the ν_2 vibration are 54 cm^{-1} and 0.06 Å, while the predicted splitting was 40 cm^{-1} using a ligand-field treatment. Their finding that the distortions are of the same order of magnitude as the relevant zero-point vibrational energies, so that no static effect can be expected, was confirmed by both Ammeter *et al.*[22] and Johannesen and co-workers,[18] revealing the dynamic nature of this distortion.

2. Methodology

2.1. Density Functional Calculations. The density functional calculations reported in this paper have been carried out with the Amsterdam Density Functional (ADF) program package.[23−25] The computational scheme is characterized by a density fitting procedure to obtain the Coulomb potential[23] and by elaborate 3D numerical integration techniques[26,27] for the evaluation of the Hamiltonian matrix elements, including those of the exchange-correlation potential. The Vosko−Wilk−Nusair parametrization[28] of electron gas data has been used for the exchange-correlation energy and potential. The molecular orbitals were expanded in an uncontracted triple-ζ STO basis set for the Cl. For V a triple-ζ 3d basis was used, augmented with one 4p polarization STO. The cores (Cl, 1s−2p; V, 1s−3p) have been kept frozen.

2.2. Calculation of the Jahn−Teller Distortion. It follows from the Jahn−Teller theorem that, at the point of the nuclear configuration where the electronic state—^{2}E presently—is degenerate, the surface of the potential energy of the nuclei in the mean field of electrons has no minimum. The question arises whether this surface possesses any minimum, and if so where it is situated. To answer this question the shape of the adiabatic potential of VCl_4 in the configuration space of the nuclear displacements Q must be determined. Symmetry considerations permit this calculation to be simplified greatly. Thus within the $3N - 6 = 9$ modes Q of VCl_4 only the normal E-type (tetragonal) displacements Q_θ and Q_ϵ are Jahn−Teller active.[1] To analyse the so-called E ⊗ e problem at hand, we follow closely the description given by I. B. Bersuker.[1] Accordingly, we first separate the totally symmetric part of the diagonal elements of the vibronic interactions, which gives rise to the force constant K_E (vide infra). Then we choose the initial configuration of the system at the point $Q_{E\gamma} = 0$, where the adiabatic potential without the vibronic interaction has a minimum, and assume that the proper anharmonicity may be neglected. Under these conditions (cf. ref 1 for more details) the two sheets of the 2-fold degenerate electronic E-term are given by the following expression:

$$\epsilon_k(Q_{E_\gamma}) = \frac{1}{2}\sum_{E_\gamma} K_E {Q_{E_\gamma}}^2 + \epsilon_k^\nu(Q_{E_\gamma}) \qquad (2.1)$$

where $k = 1$ and 2, γ represents the two components of the irrep E, and $\epsilon_k^\nu(Q_{E_\gamma})$ are the roots of the secular equation for the vibronic interaction (vide infra). From this adiabatic potential the nuclear energy spectrum and dynamics can in principle be solved.

The two electronic wave functions of the E-term may be denoted by $|\theta\rangle$ and $|\epsilon\rangle$ with symmetry properties of the two well-known functions $\theta \sim 3z^2 - r^2$ and $\epsilon \sim x^2 - y^2$ in the transition metal d functions nomenclature. We use a unique

(16) Blankenship, F. A.; Belford, R. L. *J. Chem. Phys.* **1962**, *36*, 633.
(17) Morino, Y.; Uehara, H. *J. Chem. Phys.* **1966**, *45*, 4543.
(18) Johannesen, R. B.; Candela, G. A.; Tung Tsang *J. Chem. Phys.* **1968**, *48*, 5544.
(19) Pratt, D. W. Lawrence Radiation Laboratory Report UCRL-17406; University of California: Berkeley, CA, 1967.
(20) Parameshwasan, T.; Koningstein, J. A. *J. Mol. Spectrosc.* **1977**, *66*, 350.
(21) Deiss, E. A. Undersuchungen von Elektronenstrukturen in Ubergangsmetallkomplexen. Ph.D. Dissertation, ETH Zurich, 1980.
(22) Ammeter, J. H.; Zoller, L.; Bachmann, J.; Baltzer, P.; Gamp, E.; Bucher, R.; Deiss, E. *Helv. Chim. Acta* **1981**, *64*, 1063.
(23) Baerends, E. J.; Ellis, D. E.; Ros, P. *Chem. Phys.* **1973**, *2*, 42.
(24) Baerends, E. J.; Ros, P. *Int. J. Quantum Chem.* **1973**, *2*, 42.
(25) Baerends, E. J.; Ros, P. *Chem. Phys.* **1973**, *2*, 51.
(26) Boerrigter, P. M.; te Velde, G.; Baerends, E. J. *Int. J. Quantum Chem.* **1988**, *33*, 87.
(27) te Velde, G.; Baerends, E. J. *J. Comput. Phys.* **1992**, *99*, 84.
(28) Vosko, S. H.; Wilk, L.; Nusair, M. *Can. J. Phys.* **1980**, *58*, 1200.

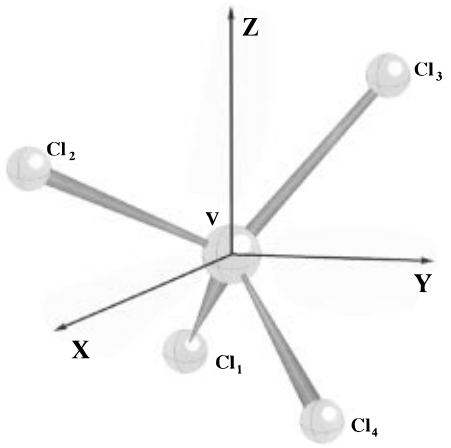

Figure 1. Coordinate system used for VCl_4. The local coordinate system of the ligands is parallel to the metal one.

coordinate system in which the *x*-, *y*-, and *z*-axes coincide with the 4-fold improper rotation axis of the tetrahedron (see Figure 1). The two components of the normal E-type displacements Q_θ and Q_ϵ are then

$$Q_\epsilon = \frac{1}{2\sqrt{2}}(-\Delta x_1 + \Delta x_2 - \Delta x_3 + \Delta x_4 + \Delta y_1 + \Delta y_2 - \Delta y_3 - \Delta y_4) \quad (2.2)$$

$$Q_\epsilon = \frac{1}{4}(+\Delta x_1 - \Delta x_2 + \Delta x_3 - \Delta x_4 + \Delta y_1 + \Delta y_2 - \Delta y_3 - \Delta y_4 - 2\Delta z_1 + 2\Delta z_2 + 2\Delta z_3 - 2\Delta z_4)$$

The elements of the vibronic interaction matrix depend only on these two coordinates. Then, retaining only the linear and second order vibronic interaction terms, the explicit form of the vibronic interaction matrix for the E ⊗ e problem is given by[1]

$$\begin{vmatrix} F_E Q_\theta + G_E(Q_\theta^2 - Q_\epsilon^2) - \epsilon^\nu & -F_E Q_\epsilon + 2G_E Q_\theta Q_\epsilon \\ -F_E Q_\epsilon + 2G_E Q_\theta Q_\epsilon & -F_E Q_\theta - G_E(Q_\theta^2 - \theta_\epsilon^2) - \epsilon^\nu \end{vmatrix} = 0 \quad (2.3)$$

where F_E and G_E denote respectively the first- and the second-order vibronic coupling constants:

$$F_E = \left\langle \theta \middle| \left(\frac{\partial V}{\partial Q_\theta}\right)_0 \middle| \theta \right\rangle \qquad G_E = \left\langle \theta \middle| \left(\frac{\partial^2 V}{\partial Q_\theta \partial Q_\epsilon}\right)_0 \middle| \epsilon \right\rangle \quad (2.4)$$

The solution of eq 2.3 yields the adiabatic potential—often denoted as "Mexican hat like"—which is correct to second order in vibronic coupling. The shape of this potential is depicted in Figure 5 (vide infra).

At this level of approximation the Jahn−Teller stabilization energy E_{JT} is

$$E_{JT} = \frac{F_E^2}{2(K_E - 2|G_E|)} \quad (2.5)$$

and the minimal barrier height between the minima is

$$\Delta = \frac{4E_{JT}|G_E|}{K_E + 2|G_E|} \quad (2.6)$$

In polar coordinates, $Q_\theta = \rho \cos\phi$, $Q_\epsilon = \rho \sin\phi$, the extreme points ($R_{JT}$, ϕ_0) of the surface are

$$R_{JT} = \frac{\pm F_E}{K_E \mp (-1)^n 2G_E} \qquad \phi_0 = n\frac{\pi}{3} \qquad n = 0, 1, ..., 5 \quad (2.7)$$

the upper and lower signs corresponding to the cases $F_E > 0$ and $F_E < 0$, respectively.

In particular it is seen from eq 2.3 that the whole E ⊗ e adiabatic energy surface is determined by solely three parameters, i.e., K_E, F_E, and G_E or, equivalently, by E_{JT} , Δ, and R_{JT}. These latter ones are easily obtained from density functional theory by using the following calculation scheme, depicted in Figure 2.

Consider a molecule with a degenerate state Γ belonging to the point group G_0. Next, among all the subgroups of G_0 determine those for which the irrep Γ, which is usually reducible in the subgroup of lower symmetry, does contain A_1. Let us denote these subgroups S_1, S_2, ... Within this set, {S_1, S_2, ...}, choose the subgroup with maximal order and call it G_1. In G_1 the state Γ will split into Γ_1, Γ_2, etc., some of which might still be degenerate. Now, we will perform two types of DF calculations with geometry optimization in G_1 symmetry: firstly, imposing G_0 symmetry to the nuclear geometry and G_1 symmetry to the electronic density; secondly, without symmetry constraints imposed on the nuclei. Both steps will be repeated for all possible combinations to generate totally symmetric electron densities in G_1.

In order to clarify this procedure, let us illustrate it with the example at hand. VCl_4 being a d_1 system, in $G_0 = T_d$ symmetry the highest occupied molecular orbital (HOMO) belongs to the irrep e and does accommodate a single electron. Inspection into a character table shows that for this example $G_1 = D_{2d}$ and the HOMO splits into a_1 and b_1. There are in this example two distinct ways to accommodate the single electron, i.e., (i) $a_1^1 b_1^0$ yielding a density ρ_1 and (ii) $a_1^0 b_1^1$ yielding another density ρ_2. Thus, four DF calculations corresponding to both of these occupations as well as to with and without geometry constraints are to be carried out. Let us denote the total energies obtained in those four calculations as follows:

$E(\rho_1,T_d)$: occupation is $a_1^1 b_1^0$, and T_d symmetry is imposed on the nuclear geometry;

$E(\rho_1,D_{2d})$: occupation is $a_1^1 b_1^0$, and the nuclear geometry has D_{2d} symmetry;

$E(\rho_2,T_d)$: occupation is $a_1^0 b_1^1$, and T_d symmetry is imposed on the nuclear geometry;

$E(\rho_2,D_{2d})$: occupation is $a_1^0 b_1^1$, and the nuclear geometry has D_{2d} symmetry

Moreover, it is easily possible to identify the symmetry-adapted nuclear displacements leading from G_0 to G_1. It has to be equivalent to those components of the irreducible tensor operators for G_0 which possess full symmetry about the distortion axis in G_1. That is, we have to identify the component $|\Gamma\gamma_{a_1}\rangle$ of G in G_0 which becomes totally symmetric in G_1.[29] This identification is most easily achieved by inspection of the Clebsch−Gordan coefficients for G_0.[30] Let us denote this

(29) Daul, C. A. Thèse d'Habilitation, University of Fribourg, 1983.
(30) Griffith, J. S. *The Irreducible Tensor Method for Molecular Symmetry Groups*, Prentice Hall International: London, 1962.

Table 1. Calculated Parameters of VCl_4

	D_{2d} compressed	D_{2d} (T_d) $^2A_1$	T_d	D_{2d} (T_d) $^2B_1$	D_{2d} elongated	exptl[a]
			Distances (Å)			
V−Cl	2.133	2.133	2.133	2.133	2.133	2.138
Cl_1-Cl_2	3.455	3.483	3.483	3.483	3.503	3.485
Cl_1-Cl_3	3.537	3.483	3.483	3.483	3.441	
			Angles (deg)			
Cl_1-V-Cl_2	108.2024	109.4712	109.4712	109.4712	110.4466	
			Total energies (eV)			
	−21.6137	−21.6074	−21.7470	−21.6084	−21.6134	

[a] Reference 17.

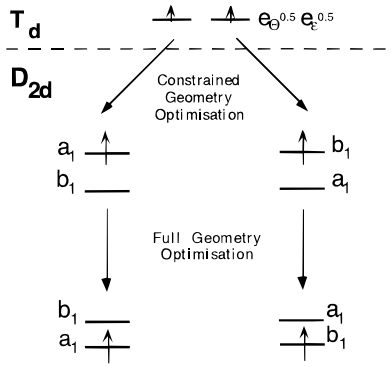

Figure 2. Schematic representation of the calculation recipe.

normal nuclear displacement as $Q\gamma_{a_1}$. For the example considered here, $Q\gamma_{a_1} = Q_\theta$. Then, using this notation, the three Jahn−Teller parameters are obtained as

$$E_{JT} = E(\rho_1,T_d) - E(\rho_1,D_{2d}) \tag{2.8a}$$

$$\Delta = \{E(\rho_1,T_d) - E(\rho_1,D_{2d})\} - \{E(\rho_2,T_d) - E(\rho_2,D_{2d})\} \tag{2.8b}$$

$$R_{JT} = Q(\rho_1, D_{2d}) \tag{2.8c}$$

It is important to remark that in DF calculations in general

$$E(\rho_1,T_d) \neq E(\rho_2,T_d) \tag{2.9}$$

This inequality is due to the very nature of the exchange-correlation functionals involved in the DF calculation.[31] We solve this problem in a pragmatic way by forcing equality of expression 2.9 as it is done in 2.8.b.

The procedure we propose here was first suggested by J. S. Griffith.[30] Due to the JT effect, the molecule undergoes a slight distortion, thus lowering its symmetry from G_0 to G_1. In this case a further operator, called the distortion operator has to be added to the molecular Hamiltonian of symmetry G_0. This operator will mimic a G_1 distortion of the G_0 ligand field. The question is how to add such a ligand field into our scheme of calculation. We do so, as indicated by Griffith, by decomposing it into a sum of components of irreps of G_0. Classifying it in terms of the point group G_0, the distortion operator will be a one-electron operator which is a sum of those components of the irreducible tensor operators for the group G_0 which possess full symmetry about the distortion axis in the point group of lower symmetry G_1. This is essentially the theoretical foundation of our calculation recipe. In fact, it can easily be shown to yield the same result as the conventional procedure to select the JT active mode. In this case the Hamiltonian is expanded as

$$H_1 = H_0 + \sum_{k=1}^{3n-6}\left(\frac{\partial H}{\partial Q_k}\right)_0 Q_k \tag{2.10}$$

and the application of group theoretical rules to

$$\left\langle \Gamma m_\Gamma \left| \frac{\partial H}{\partial Q_k} \right| \Gamma m'_\Gamma \right\rangle \tag{2.11}$$

yields the JT active mode: $Q\gamma_{a_1}$.

3. Results and Discussion

In this article, we applied the method described in the previous section to investigate the Jahn−Teller distortion on VCl_4. The coordinate system used is shown in Figure 1. The calculations executed are represented schematically in Figure 2.

As a starting point, VCl_4 has also been optimized in T_d symmetry. Here the single electron is occupying the degenerate e orbitals. Within DFT, one can state that both e orbitals carry 0.5 electron, leading to a totally symmetric electron distribution (ρ_0). This is denoted in Figure 2 with $e_\theta^{0.5}$ $e_\epsilon^{0.5}$. The second step in the calculation scheme is occupying selectively one of the two degenerate e orbitals, but staying at T_d geometry. This is done by imposing, within the ADF program, D_{2d} symmetry onto the system. Hereby the two e orbitals are split up into an a_1 and a b_1 orbital, which are populated as $^2A_1$ (=ρ_1) and $^2B_1$ (=ρ_2) in two separate calculations. T_d geometry is preserved by imposing the angle Cl−V−Cl to stay at 109.471°. So here a constrained geometry optimization is carried out, giving rise to the energies $E(\rho_1,T_d)$ and $E(\rho_2,T_d)$. The final step in the calculation recipe is performing a complete (=no constraints) geometry optimization on both of the D_{2d} cases, leading to two different geometries and the energies $E(\rho_1,D_{2d})$ and $E(\rho_2,D_{2d})$.

The obtained geometric parameters for the regular (T_d) as well as the distorted (D_{2d}) conformations are presented in Table 1, along with the corresponding total energies. Comparing the parameters for the T_d geometry with the gas electron diffraction data[17] shows us a good agreement with the experiment, giving a difference of 0.005 Å for the distance V−Cl, and 0.002 Å for d(Cl−Cl).

Table 1 documents that, only due to the imposal of a different electron distribution in the two D_{2d} cases, the calculations give rise to a simulation of the JT distortion. The results show us a change in angle of 1.268° for the compression and 0.975° for the elongation. The distance V−Cl turns out to be only slightly changed with a difference of less than 0.001 Å in both cases.

Considering the energies, we notice first of all, as already depicted in expression 2.9, that the energies $E(\rho_1,T_d)$ and $E(\rho_2,T_d)$ are not equal. A difference of 12 cm^{-1} between them is observed. This is due to the nature of the exchange-correlation functional involved in the DF calculations.[31] Sec-

(31) Daul, C. A.; Doclo, K.; Stückl, C. A. In *Recent Advances in Density Functional Methods, Part II*; Chong, D., Ed.; World Scientific Publishing Company: Singapore, in press.

Table 2. Jahn−Teller Parameters for VCl_4

method	R_{JT} (Å)	E_{JT} (cm^{-1})	Δ (cm^{-1})
crystal field[a]	0.381	250	
ligand field[b]	−0.07	14	
angular overlap[c]		119(43)	
EHMO[d]	0.032	6	
exptl[e]	0.16(6)	18	
present work			
recipe[f]	0.078	51	10.5
energy surface fit	0.079	52	12

[a] Reference 9. [b] Reference 11. [c] Reference 29. [d] Reference 21. [e] References 17, 18. [f] Equations 2.8.

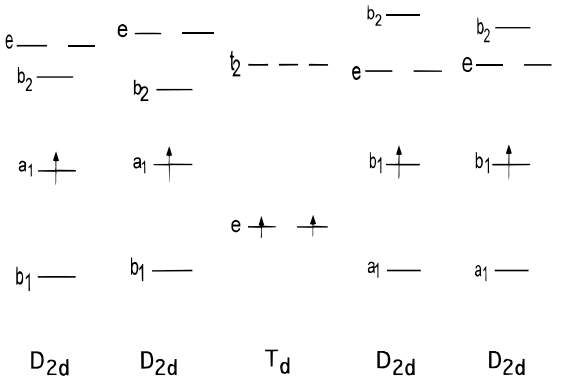

Figure 3. HOMO−LUMO scheme for the different conformations

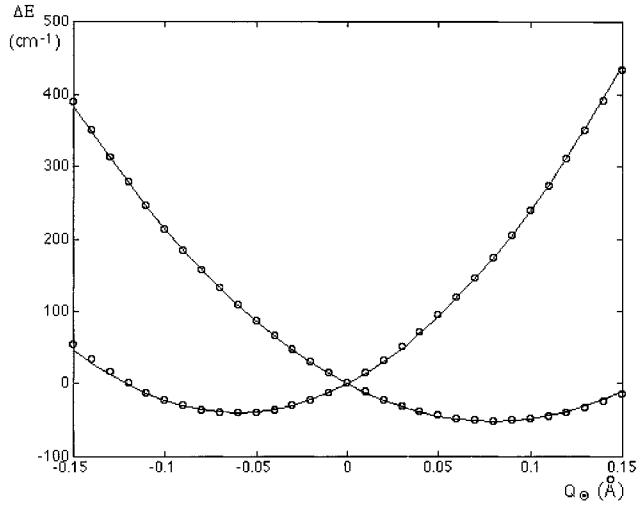

Figure 4. Adiabatic energy surface of the two sheets of the 2-fold degenerate electronic E-term (cf. eq 2.1) in cm^{-1} versus Q_θ in Å (cf. eq 2.2). The curve on the left-hand side corresponds to the $a_1^1b_1^0$ occupation. The one on the right-hand side corresponds to $a_1^0b_1^1$. The line (−) corresponds to the fitted model, and the circles (○) to DF calculations.

ondly, it becomes clear why the two D_{2d} calculations constraining the T_d geometry are also performed. Comparing the final D_{2d} energies only with the obtained energy from the T_d calculation would give a misleading result. The electron distribution in the nondistorted VCl_4 is different from that in VCl_4 (D_{2d}). Hence the electron interaction terms in the total energy are also different. In order to compare the two distorted conformations with the one in higher symmetry, the unpaired electron must be distinguishably placed in one of the two degenerate orbitals.

From the results of the complete calculation scheme, i.e., the changes in geometry and energy, the three JT parameters, E_{JT}, R_{JT}, and Δ, can be easily derived following the expressions 2.8.a−c. The obtained values are tabulated in Table 2, along with the values obtained from the full energy surface calculation

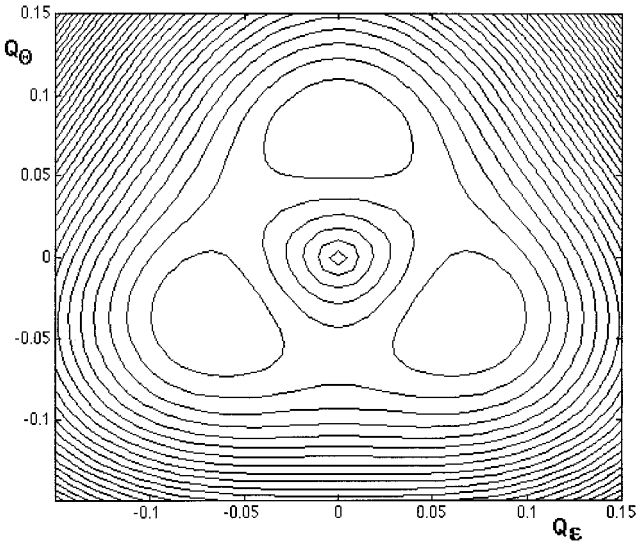

Figure 5. : Contour plot of the lower sheet of the adiabatic potential of the E ⊗ e problem of VCl_4 in the space of Q_θ and Q_ϵ coordinates.

(vide infra). Also the experimental parameters and results from other calculation methods are included. The results indicate two very shallow minima, confirming the dynamic character of the Jahn−Teller effect. We see here also that the two minima of the energy surface do not have the same depth, indicating a different stability and hence preference of the system for the two conformations. This was also found by Johannesen.[18]

A partial MO scheme, resulting from the DF calculations, is shown in Figure 3. The fact that immediately catches the eye is the orbital order in the final D_{2d} conformations. The semi occupied MO stays, after the energy minimization, above the lowest empty orbital. This is somewhat surprising in light of the usual idea we have about the Jahn−Teller effect, namely, the splitting of the degenerate orbitals and occupying of the lowest one. But what we should keep in mind here is that the JT effect is a change in geometry due to the lowering of the *total* energy. This means that the Kohn−Sham eigenvalues do not neccesarily reflect this. It is well-known that, in DFT, the total energy is not equal to the sum of the Kohn−Sham orbitals.

We have also carried out a full energy surface calculation along the normal displacements coordinate Q_θ in D_{2d} symmetry for both electronic states: $^2A_1$ and $^2B_1$. Least squares analysis of this data yields a very good fit with a standard deviation of the estimated energy of 2 cm^{-1}. The following values are obtained for the model parameters:

$$K_E = 19084 \pm 100 \text{ cm}^{-1} \text{ Å}^{-2}$$

$$F_E = 1311 \pm 6 \text{ cm}^{-1} \text{ Å}^{-1}$$

$$G_E = 1260 \pm 50 \text{ cm}^{-1} \text{ Å}^{-2}$$

Substituting these results into eqs 2.5−2.7 yields

$$E_{JT} = 52 \text{ cm}^{-1}$$

$$\Delta = 12 \text{ cm}^{-1}$$

$$R_{JT} = 0.0792 \text{ Å}$$

The result of these calculations is depicted in Figure 4. With these parameters and the second-order vibronic coupling model described in section 2.2, the "Mexican hat like" plot, shown in Figure 5, is constructed. Looking at the JT parameters obtained

in the present work, we see that the results from the proposed calculation recipe are in even better agreement with the experiment than the ones obtained from the potential energy surface scan. But both show to overestimate the E_{JT} compared to the experimental value.

4. Conclusion

The results obtained in this work demonstrate once more the good ability of DFT calculations to predict the state energies as well as the corresponding structural parameters with a reasonable accuracy.

A useful extension to this work would be the systematic calculation of the Jahn−Teller distortions of more complexes with different molecular symmetries. The evaluation of these properties could easily be undertaken within the same methodological frame in the near future.

Acknowledgment. This work is part of Project 20-40′638.94 of the Swiss National Science Foundation. Also the authors wish to thank Prof. Evert Jan Baerends and Dr. B. te Velde for helpful discussions on the lack of degeneracy of the two E components in tetrahedral symmetry when using ADF in particular and DFT in general. P.T.M. thanks the Council of Scientific and Industrial Research, India.

IC961220+